

Article

Assessing Climate Change Impacts on River Flows in the Tonle Sap Lake Basin, Cambodia

Chantha Oeurng^{1,3}, Thomas A. Cochrane^{2,*}, Sarit Chung¹, Mathias G. Kondolf^{3,4},
Thanapon Piman⁵ and Mauricio E. Arias⁶

¹ Faculty of Hydrology and Water Resources Engineering, Institute of Technology of Cambodia, Phnom Penh 12156, Cambodia; chanthaposat@yahoo.com (C.O.); sarithchung168@gmail.com (S.C.)

² Department of Civil and Natural Resources Engineering, University of Canterbury, Christchurch 8140, New Zealand

³ Department of Landscape Architecture and Environmental Planning, University of California, Berkeley, CA 94720, USA; kondolf@berkeley.edu

⁴ Collegium—Institute of Advanced Studies, University of Lyon, 69007 Lyon, France

⁵ Stockholm Environment Institute, Asia Center, Bangkok 10330, Thailand; thanapon.piman@sei.org

⁶ Department of Civil and Environmental Engineering, University of South Florida, Tampa, FL 33620, USA; mearias@usf.edu

* Correspondence: tom.cochrane@canterbury.ac.nz

Received: 3 February 2019; Accepted: 19 March 2019; Published: 25 March 2019



Abstract: The Tonle Sap is the most fertile and diverse freshwater ecosystem in Southeast Asia, receiving nurturing water flows from the Mekong and its immediate basin. In addition to rapid development in the Tonle Sap basin, climate change may threaten natural flow patterns that sustain its diversity. The impacts of climate change on river flows in 11 sub-basins contributing to the Tonle Sap Lake were assessed using the Soil and Water Assessment Tool (SWAT) model to quantify the potential magnitude of future hydrological alterations. Projected river flows from three General Circulation Models (GFDL-CM3, GISS-E2-R-CC and IPSL-CM5A-MR) for three time horizons (2030s, 2060s and 2090s) indicate a likely decrease in both the wet and dry season flows. The mean annual projected flow reductions range from 9 to 29%, 10 to 35% and 7 to 41% for the 2030s, 2060s and 2090s projections, respectively. Moreover, a decrease in extreme river flows (Q_5 and Q_{95}) was also found, which implies there could be a decline in flood magnitudes and an increase in drought occurrences throughout the basin. The results of this study provide insight for water resources planning and adaptation strategies for the river ecosystems during the dry season, when water flows are projected to decrease.

Keywords: climate change; river flow; Tonle Sap; SWAT model; Lower Mekong

1. Introduction

Climate change is an important part of the challenges of sustainable development in developing countries. Climate change represents one of the greatest environmental, social and economic threats facing the world today [1]. Future changes in river flow and watershed hydrology that are caused by one of the drivers such as climate change, have become increasingly important topics for water resource management. Developing countries are faced with immediate concerns that relate to land degradation, freshwater shortages, food security, and air and water pollution. Climate change will exacerbate these concerns, leading to further water shortages, land degradation and desertification [1]. Across Southeast Asia, the mean annual temperature by the end of the 21st century is expected to rise from 0.8 °C in the lowest emissions scenario to 3.2 °C in the highest emissions scenario, while a moderate increase in precipitation is also projected for this region, from 1% to 8% by 2100 [2]. With rising temperatures and increasing rainfall, increased river discharge and flooding are predicted

during the wet season, while extended droughts are likely to occur during the dry season. The study of the potential streamflow changes associated with future climate change scenarios is of practical significance for local socio-economic development and eco-environmental protection [3,4]. Since it is difficult to detect how hydrological regimes may actually be changing, Bates et al. [5] recommend that a scenario-based approach to water management should be adopted. A set of scenarios known as the Representative Concentration Pathways (RCPs), published in the Fifth Assessment Report of the Intergovernmental Panel on Climate Change (IPCC) [6], are suited to providing a wide range of possible emission scenarios. The RCPs incorporate various scenarios of policy-level interventions, adaptations and vulnerability mitigation practices [7]. These emission scenarios, together with a range of viable (GCM) models, allow for a comprehensive understanding of the impacts of climate change on water resources.

The effective planning of water resource use and protection under changing environmental conditions requires the use of hydrological models that can simulate flow regimes under different scenarios of change. Therefore, various hydrological models have been developed to provide a link between change scenarios and water yields, through the simulation of hydrologic processes within watersheds. Examples of these hydrological models are the Agricultural Non-Point Source (AGNPS) [8], Hydrological Simulation Program-FORTRAN (HSPF) [9], MIKE SHE [10], Soil and Water Assessment Tool (SWAT) [11] and Agricultural Policy/Environmental Extender (APEX) [12]. Among these models, the SWAT model is the most widely used model, and it has been applied in different regions to analyse a wide range of hydrological problems, including potential changes to the streamflow under future climate scenarios. More than 1000 peer-reviewed articles related to the use of the SWAT have been published, which include studies of hydrological responses to climate change [13]. In the Mekong basin, Piman et al. [14] applied the SWAT model for the management of hydropower under climate change in a key tributary of the Mekong, which showed that climate change can influence hydropower operations. Shrestha et al. [15] also assessed the uncertainty in flow and sediment projections, due to future climate scenarios, using SWAT for the 3S Rivers in the Mekong Basin. Oeurng et al. [16] also applied SWAT to evaluate the impact of climate changes in riverine nitrate in the Sesan, Srepok, and Sekong tributaries of the Lower Mekong River Basin. Moreover, the SWAT model was used to simulate the streamflow in the Indrawati River Basin, Nepal, and to analyse the hydrological response to climate change [17]. Another study of climate change impacts on the seasonality of water resource was conducted in the Ca river basin, a shared boundary river between Laos and Vietnam [18]. The SWAT model was also applied, to investigate the impacts of climate change on flow regimes in the Chao Phraya River Basin, Thailand [19], and integrated with a Statistical DownScaling Model (SDSM) for estimating river flow responses to climate change in the Lake Dianchi watershed, China [20].

Over the last few decades, water resources in the Tonle Sap basin have been affected by rapid population growth, urbanization, deforestation, agricultural expansion and hydropower demand. In addition, Cambodia is also expected to be seriously affected by the impacts of climate change, due to the high dependency of the economy on the agriculture sector, which sustains the livelihood of approximately 80% of the total population. The effects are likely to include an increased frequency of severe water scarcity and flooding, resulting in crop failures and food shortages [21].

To properly manage water resources in Cambodia, it is crucial to understand the current and future river flow characteristics of each sub-basin within the Tonle Sap Basin. So far, there has been limited monitoring and hydrological modelling of the potential climate change impacts on flows in tributaries to Tonle Sap Lake, due to limitations in the capacity and resources of national institutions. Most studies have focused on the Mekong mainstream and reverse flows to Tonle Sap Lake [22–25]. Kummur et al. [26] reported that the majority (53.5%) of the water originates from the Mekong mainstream, but the lake's tributaries also play an important role, contributing 25–30% of the annual flow, while 12.5% is derived from precipitation. The sub-basins clearly play a prominent role in maintaining dry-season lake levels, but they have been poorly monitored and studied. There is

thus a need to understand the effect of climate change, and the ongoing developments in the flow contributions from tributary basins to the Tonle Sap.

Therefore, the main objectives of this study were to: (1) simulate baseline river flows in all 11 Tonle Sap sub-basins, and (2) to assess the potential impacts of future climate change on river flows within each sub-basin, using a calibrated SWAT model with projected future climate change scenarios.

2. Materials and Methods

2.1. Study Area

The Tonle Sap Lake Basin consists of the Tonle Sap Lake and 11 major tributaries, with a total catchment area of 86,000 km² (Figure 1a). Located in Kampong Thom Province, Stung Sen is the largest tributary, with an area of 16,341 km², and contributes the highest flows. Detailed information on land use (2010), annual average river flow, and the catchment area of each sub-basin in the lake basin are presented in Table 1. The average annual rainfall varies from 1000 to 1500 mm. The majority of the basin consists of lowlands with elevations of less than 100 m above the mean sea level, and with gentle slopes (Figure 1b). Elevations increase in the southwest in the Cardamom Mountains, to over 1700 m. The steep escapement of the chain of the Dangrek Mountains reaches an average level of 500 m in the north (Figure 1b). There are 10 main soil types (Figure 1c) within the Tonle Sap Basin. The land cover is dominated by 55% forest land (of which 3% is flooded forest) and 45% agricultural land [27] (Figure 1d).

The Tonle Sap Lake (the “Great Lake”) flows into the Mekong River via the 120 km long Tonle Sap River. The Tonle Sap’s unique hydrology results from seasonally bi-directional flow: during the dry season, water flows from the Tonle Sap Lake to the Mekong River, and during the flood season (between June and October), the water level is higher on the Mekong River than in the lake, forcing the water to flow backward through the Tonle Sap River into to Tonle Sap Lake, inundating its floodplain and causing the surface area of the lake to swell from 2600 km² to 12,000 km² [26,28]. The water level of the Tonle Sap Lake varies from an average depth of less than 2 m in the dry season to over 10 m in the flood season. During the wet season, the surface area of the lake can expand to 3–4 times its dry season extent, resulting in the most productive ecosystem and fishery within the Mekong River Basin [28,29]. Around 34% of Tonle Sap Lake’s waters originate from the Tonle Sap drainage basin, while about 53.5% of the lake’s waters originate from the Mekong River, and 12.5% is derived from precipitation. [26]. This distribution, however, is highly seasonal, as the Tonle Sap system is fed exclusively by its 11 tributaries for approximately six months (November through May) every hydrological annual cycle.

Table 1. Sub-basin areas, land-use, and mean annual flows to the Tonle Sap.

N ^o	Sub-basin	Area (km ²)	Forest Land	Agricultural Land	Urban Land
1	ST. Chinit	8235	62.70%	37.26%	0.04%
2	ST. Sen	16,341	85.37%	14.61%	0.02%
3	ST. Staung	4356	75.03%	24.97%	0.00%
4	ST. Chikreng	2713	78.38%	21.62%	0.00%
5	ST. Siem Reap	3618	26.28%	73.57%	0.15%
6	ST. Sreng	9930	61.68%	38.32%	0.00%
7	ST. Mongkol Borey	10,856	14.67%	85.14%	0.19%
8	ST. Sangke	6051	53.76%	46.09%	0.14%
9	ST. Dauntri	3695	43.42%	56.58%	0.00%
10	ST. Pursat	5963	76.15%	23.76%	0.09%
11	ST. Baribo	7152	25.01%	74.61%	0.39%

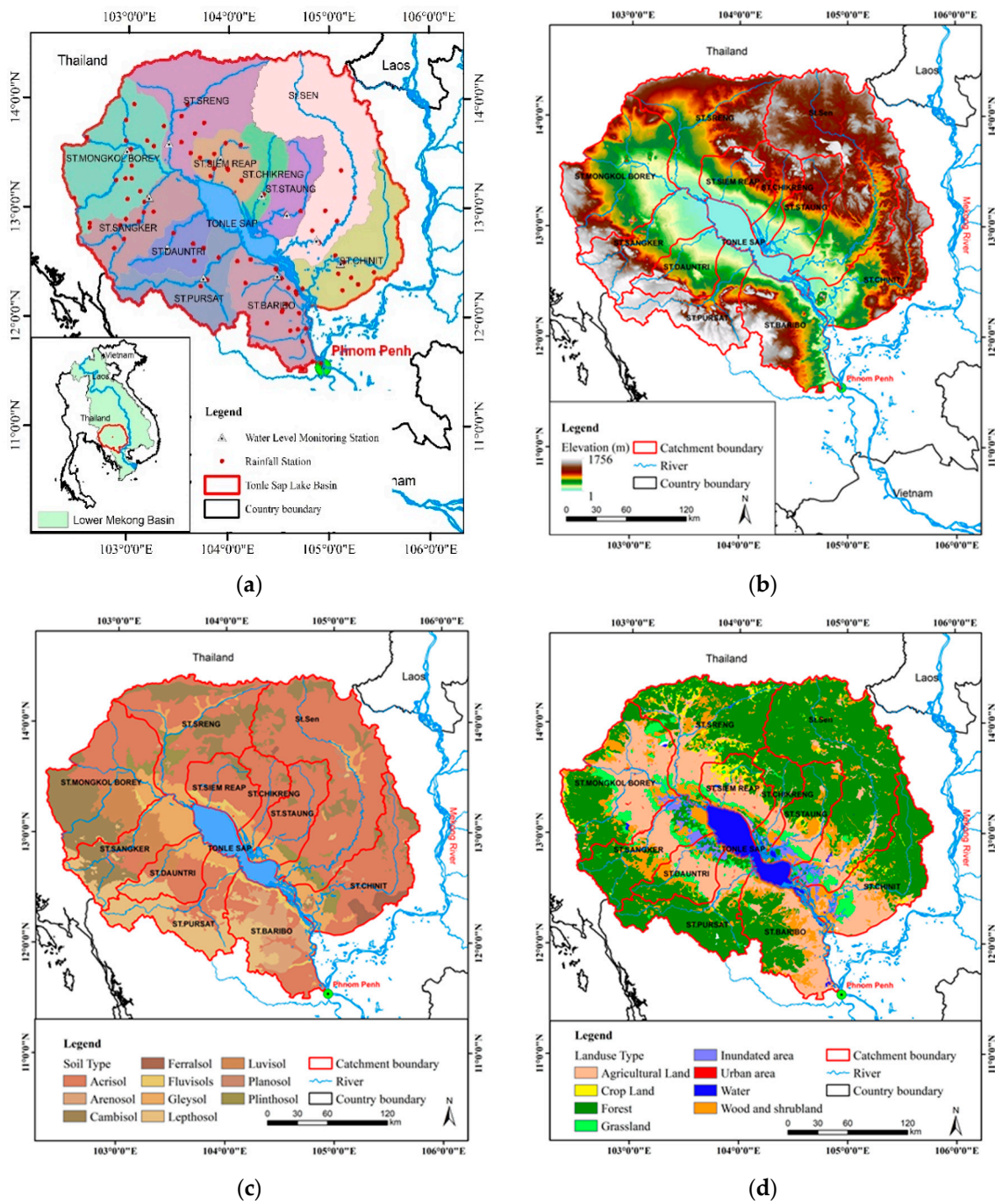


Figure 1. (a) Study area with water level monitoring and rainfall stations, (b) digital elevation model, (c) soil type and (d) land use/land cover of Tonle Sap Lake Basin.

2.2. River Flow Data

Water level data were collected by the Department of Hydrology and River Works, Ministry of Water Resources and Meteorology, Cambodia, at the river gauging stations in each tributary outlet (Appendix A Table A1). For each tributary, the flows were calculated from the observed water levels using the rating curves developed for each station. The basic statistics of river flow in each river are presented in Table 2.

Table 2. Basic statistics of the river flow and annual rainfall of Tonle Sap River Basin.

N°	River Name	Flows (m ³ /s)				Annual Rainfall (mm)			
		Min	Mean	Max	STDV	Min	Mean	Max	STDV
1	ST. Chinit	0.06	65	601	80	1058	1453	1839	181
2	ST. Sen	0.1	249	1476	320	1104	1385	1839	176
3	ST. Staung	0.01	28	277	51	1125	1470	1924	195
4	ST. Chikreng	0.01	11	395	38	964	1271	1646	150
5	ST. Siem Reap	0.04	6	132	10	1028	1286	1553	137
6	ST. Sreng	0.01	45	340	74	1138	1336	1560	125
7	ST. Mongkol Borey	0.3	18	303	35	1261	1487	1749	135
8	ST. Sangke	0.67	62	1020	98	1109	1390	1664	154
9	ST. Dauntri	0.05	4	260	12	832	1151	1652	197
10	ST. Pursat	0.01	83	1264	121	1103	1493	2031	209
11	ST. Baribo	0.02	27	287	30	1038	1303	1568	152

2.3. Modelling Approach

The SWAT model is a semi-physically based model that is designed to simulate the impact of land management practices on the environmental–hydrological system in a watershed over long periods (years to decades). The SWAT model allows for a number of different physical processes to be simulated in a watershed, including water movement, sediment movement, crop growth, and nutrient cycling [30]. SWAT can be used to analyse small or large catchments by discretising them into sub-basins, which are then further subdivided into hydrological response units (HRUs) with homogeneous land uses, soil types, and terrain slope class.

SWAT considers the watershed hydrology in two phases: the land phase and routing phase. The land phase is composed of the watershed land areas that simulate the water that is transported to the channels, together with sediment, nutrients and pesticides. The routing phase comprises of the behaviour of the water in the channels, from the tributaries to the watershed outlet. The hydrology cycle that is simulated by the SWAT model is based on the following water balance equation (Equation (1)):

$$SW_t = SW_0 + \sum_i^t (R_{day} - Q_{surf} - E_a - W_{seep} - Q_{gw}) \quad (1)$$

where, SW_t is the final soil water content (mm H_2O), SW_0 is the initial soil water content on day i (mm H_2O), t is the time (days), R_{day} is the amount of precipitation on day i (mm H_2O), Q_{surf} is the amount of surface runoff on day i (mm H_2O), E_a is the amount of evapotranspiration on day i (mm H_2O), W_{seep} is the amount of water entering the vadose zone from the soil profile on day i (mm H_2O) and Q_{gw} is the amount of groundwater exfiltration on day i (mm H_2O).

SWAT simulates runoff by using the SCS (Soil Conservation Service) curve number method and the Green–Ampt infiltration method. The peak runoff rate is estimated by using a modification of the Rational Method. Water is routed through the channel network by using the variable storage routing method, or the Muskingum routing method. The groundwater flow contribution to the total river flow is simulated by creating a shallow aquifer storage area [31], whereby percolation from the root zone is recharged to the shallow aquifer. Three methods for estimating potential evapotranspiration are used in SWAT: Priestley–Taylor [32], Penman–Monteith [33] and ET–Hargreaves [34]. A full explanation of the SWAT theories and structure are given in the SWAT theoretical documentation [30]. In this study, the SCS curve number and Muskingum routing methods were used for surface runoff and flow computations while the Penman method was used to estimate potential evapotranspiration.

2.4. SWAT Model Input

The following spatial data were used in this study:

1. A digital elevation model (DEM) with a 50 m horizontal resolution for the lower Mekong (Figure 1b). This DEM came from historical scanned map sheets, and the contours were selectively vectorised by the Mekong River Commission (MRC).
2. A soils map developed by the MRC from base maps at 1:250,000 scale, based on the FAO/UNESCO 1988 classification; up to three levels and 10 main soil types were included in the model.
3. A land-use/land-cover (LULC) map developed by the MRC, based on satellite imagery from 1993–1997. LULC was characterized, and it included eight major LULC classes (Figure 1d).

The daily time-series of the observed rainfall data from 1985 to 2015 was used to generate a daily time-series of average sub-basin rainfall, for each of the SWAT sub-basins, using the MQUAD method [35], by fitting a multi-quadratic surface to the daily rainfall data at all relevant locations in and around the study area, and then integrating this over each sub-basin area to obtain the average daily rainfall for the sub-basin. The process was repeated for each day of recording. At each time-step, the availability of weather data at each rainfall station was verified. If the data at an individual rainfall station was missing, it was excluded from the analysis for that time-step, and the multi-quadratic surface was only fitted to the available data. Climatological data (temperature, evaporation, humidity, wind speed and solar radiation) were obtained from observed stations within the basin.

2.5. Model Calibration and Validation

The SWAT model was calibrated and validated for river flow. The daily flows were calibrated (1997–2003) and validated (2004–2015) at 11 different river flow monitoring stations. The parameters for the flow simulations were fitted through an auto-calibration procedure, using SWAT-CUP for the 11 river flow stations. The daily flow calibration from 1997 to 2003 was also carried out using a sequential uncertainty fitting algorithm (SUFI-2) with SWAT-CUP [36]. The initial parameter ranges for optimization were based on the likely maximum range recommended for each parameter, by the SWAT and SWAT-CUP developers for the conditions in the basin (Appendix A Table A2). The Nash–Sutcliffe model efficiency factor (*NSE*) was used as the objective function.

2.6. Model Performance Evaluation

The performance of the model in stream flow was evaluated graphically and by the Nash–Sutcliffe efficiency (*NSE*), the coefficient of determination (R^2), the percent bias (*PBIAS*), and the root mean squared error observations standard deviation ratio (*RSR*):

$$NSE = 1 - \frac{\sum_{i=1}^n (O_i - S_i)^2}{\sum_{i=1}^n (O_i - \bar{O}_i)^2} \quad (2)$$

$$R^2 = \frac{\sum_{i=1}^n (O_i - \bar{O}_i)(S_i - \bar{S}_i)}{\left[\sum_{i=1}^n (O_i - \bar{O}_i)^2 \right]^{0.5} \left[\sum_{i=1}^n (S_i - \bar{S}_i)^2 \right]^{0.5}} \quad (3)$$

$$PBIAS = \frac{\sum_{i=1}^n (O_i - S_i)}{\sum_{i=1}^n O_i} \quad (4)$$

$$RSR = \frac{\sqrt{\sum_{i=1}^n (O_i - S_i)^2}}{\sqrt{\sum_{i=1}^n (O_i - \bar{O}_i)^2}} \quad (5)$$

where O_i and S_i are the observed and simulated values, n is the total number of paired values, \bar{O}_i is the mean observed value and \bar{S}_i is the mean simulated value. NSE is a normalized statistic that compares the residual variance with the observed data variance [37].

NSE ranges from negative infinity to 1, with 1 denoting perfect agreement between the simulated and observed values. High positive values of NSE indicate a better model simulation, while negative NSE indicates that the observed mean is a better predictor than the model being used. NSE shows how well the plot of the observed versus predicted data fits the 1:1 line. However, a shortcoming of the Nash–Sutcliffe statistic is that it does not perform well in periods of low flow, as the denominator of the equation tends to zero, and NSE approaches negative infinity with only minor simulation errors in the model.

2.7. Climate Scenarios and Downscaling

The development of climate change scenarios was based on multiple Global Circulation Models (GCMs), emission scenarios, time horizons and locations [38]. Uncertainty associated with the different GCMs has been previously identified as the most significant source of uncertainty in flow and sediment modelling [15]. Therefore, the GCM selection of the climate change scenario development procedure is the most important factor. Based on the study by MRC [38], three GCMs (GISS-E2-R-CC, IPSL-CM5-MR and GFDL-CM3) and the medium-emission scenarios of Representative Concentration Pathways (RCP6.0) were considered for the general impacts of climate change. Three time horizons (near-term future 2021–2040, medium-term future 2051–2070, long-term future 2081–2100) were considered in this study, as these time horizons are being used by the MRC in other planning contexts.

Downscaled climate change data sets (IPCC 5th Assessment Report) were obtained from the MRC Climate Change and Adaptation Initiative (CCAI). This dataset includes the SWAT model ready monthly ‘change factors’ for precipitation, temperature, solar radiation and relative humidity. MRC CCAI uses SIMCLIM software to downscale the climate. SimCLIM uses pattern scaling plus bilinear interpolation algorithm to downscale the GCM outputs. MRC CCAI uses change factors to quantify the projected alterations to climate, because the change factor approach represents the simplest and most practical way to produce scenarios based on multiple GCMs, emission scenarios, sensitivities, time horizons and locations [38].

2.8. Analysing River Flow Changes

Two techniques were employed to analyse different aspects of flow changes under GCMs for RCP6.0. The first technique was to analyse the changes in seasonal and annual variability of monthly flows. The average monthly flow and the percentage change of the annual flow were calculated and used to understand changes in the river’s flow regime. The second technique was to analyse the hydrological extremes. Daily Q_5 and Q_{95} were calculated, to analyse changes in high-flow and low-flow conditions, respectively. A flow duration curve was developed to identify the Q_5 and Q_{95} . These results were analysed at the sub-basin scale for a period of 31 years (1985–2015).

3. Results and Analyses

3.1. Performance of the Hydrological Simulations

The model was calibrated for the 1997–2003 period, and validated with available data from 2004 up to 2015 for the 11 hydrological stations at the outlet of each sub-basin, and the Nash–Sutcliffe efficiency and R^2 for both daily and monthly values were compared. Through the automatic calibration process

(SUFI), 19 parameter values were fitted to the observed data (Appendix A Table A2). Calibration and validation performances for monthly flows were satisfactory ($NSE > 0.5$) for most of the rivers, except for the Chikreng, Dauntri and Sangke Rivers (Tables 3 and 4). In general, both the observed and predicted hydrographs had a similar seasonal and interannual pattern for all 11 sub-basins of the Tonle Sap; however, the SWAT model has been shown to overestimate peak flows (Figure 2). Scatter plots between the simulated and observed river flows for the calibration and validation periods for daily and monthly values showed similar patterns (Appendix A Figure A1). The hydrological simulations did not perform well for basins such as Chikreng and Dauntri, because of data scarcity and inaccuracy in rainfall, and the estimated discharge in those basins. Given the budget constraints and the low investment in water infrastructure in those basins, the water resources ministry of Cambodia has not been able to invest in water resources and rainfall monitoring at those locations.

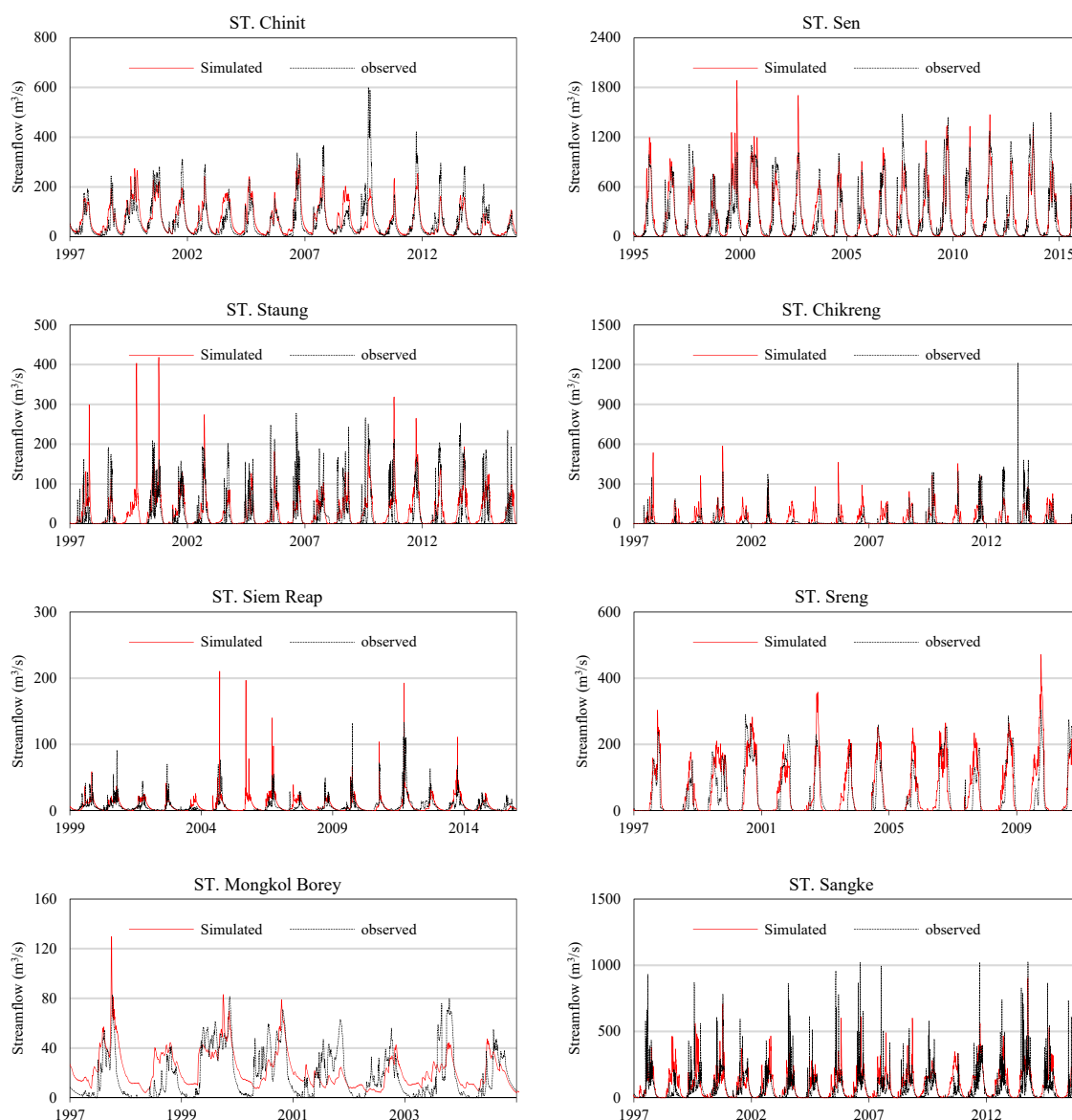


Figure 2. Cont.

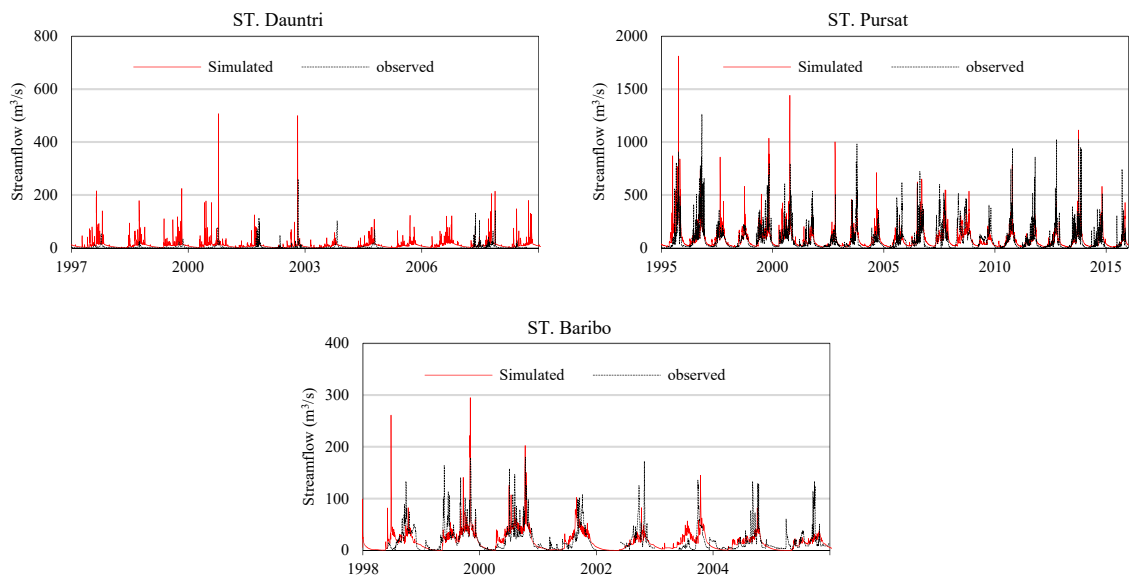


Figure 2. Comparison between daily observed and simulated river flows in 11 sub-basins of Tonle Sap Lake Basin.

The mean annual river flow simulated in each sub-basin of Tonle Sap Basin for the baseline period is presented in Figure 3, with the Sen River showing the highest mean annual flows.

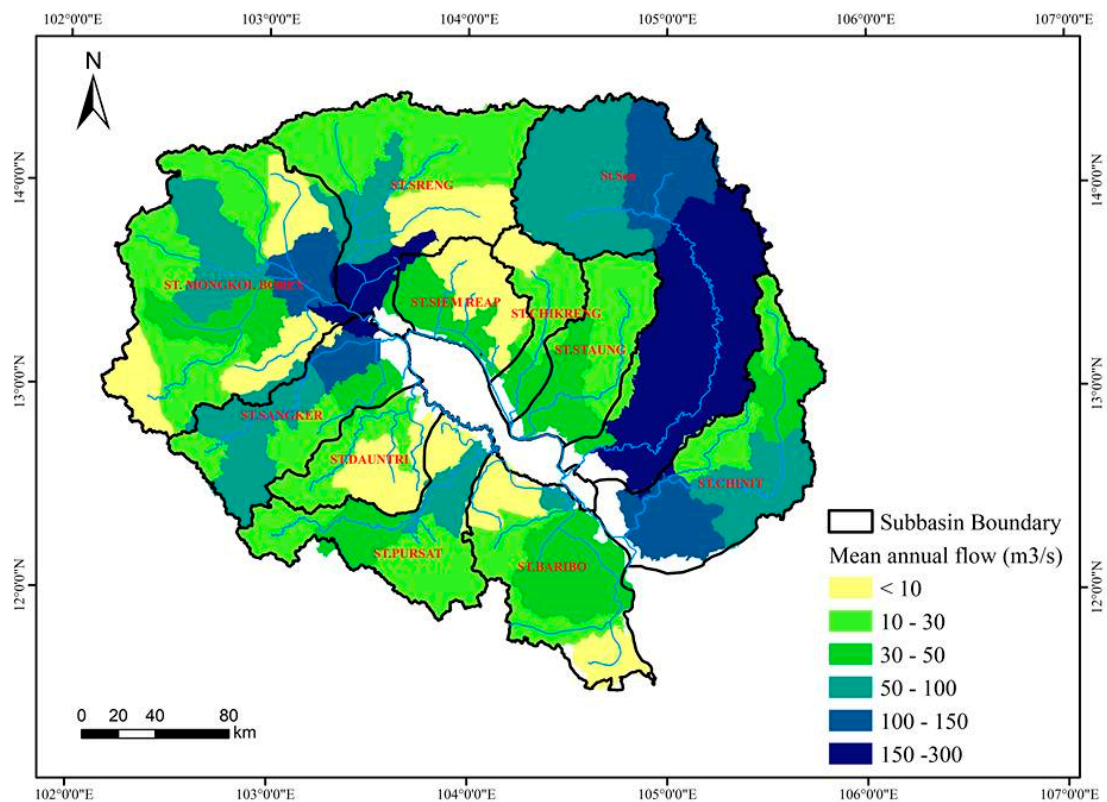


Figure 3. Spatial distribution of the (mean annual) river flow in each sub-basin, simulated from the Soil and Water Assessment Tool (SWAT) model (1985–2015).

Table 3. Calibration and validation performance for daily time-step simulations at all 11 rivers in Tonle Sap Lake Basin showing the Nash-Sutcliffe efficiency (NSE), percent bias (PBIAS), root mean squared error observations standard deviation ratio (RSR), and coefficient of determination (R^2).

River	Station Name	Calibration Period	NSE	PBIAS	RSR	R^2	Validation Period	NSE	PBIAS	RSR	R^2
ST. Chinit	Kampong Thmar	1997–2003	0.71	−0.20	0.54	0.75	2004–2015	0.59	0.01	0.64	0.59
ST. Sen	Kampong Thom	1995–2003	0.71	−0.13	0.54	0.74	2004–2015	0.81	0.03	0.44	0.81
ST. Staung	Kampong Chen	1997–2003	0.35	−0.18	0.81	0.45	2004–2015	0.53	−0.06	0.69	0.53
ST. Chikreng	Kampong Kdei	1997–2003	−1.61	−1.95	1.61	0.29	2004–2015	0.08	−0.90	0.96	0.30
ST. Siem Reap	Prasat Keo	1999–2003	0.35	−0.17	0.80	0.41	2004–2015	0.31	−0.02	0.83	0.37
ST. Sreng	Kralanh	1997–2003	0.60	−0.21	0.63	0.70	2004–2011	0.65	−0.27	0.59	0.74
ST. Mongkol Borey	Sisophon	1997–2003	0.38	−0.22	0.78	0.44	2004	0.29	−0.27	0.84	0.38
ST. Sangke	Battambang	1997–2003	0.02	−0.30	0.99	0.26	2004–2015	0.09	−0.62	0.95	0.38
ST. Dauntri	Prek Chik	1997–2003	−4.02	−2.32	2.24	0.04	2004, 2007–2008	−1.55	−1.30	1.60	0.06
ST. Pursat	Bac Trakuon	1995–2003	0.29	−0.09	0.84	0.36	2004–2015	0.45	0.01	0.74	0.45
ST. Baribo	Baribo	1998–2003	0.25	0.02	0.86	0.33	2004–2005	0.27	0.20	0.85	0.30

Table 4. Calibration and validation performance (NSE, PBIAS, RSR, and R^2) for monthly time step simulation at all 11 rivers in Tonle Sap Lake Basin.

River	Station Name	Calibration Period	NSE	PBIAS	RSR	R^2	Validation Period	NSE	PBIAS	RSR	R^2
ST. Chinit	Kampong Thmar	1997–2003	0.74	−0.20	0.51	0.78	2004–2015	0.61	0.01	0.62	0.61
ST. Sen	Kampong Thom	1995–2003	0.80	−0.13	0.45	0.82	2004–2015	0.87	0.03	0.37	0.87
ST. Staung	Kampong Chen	1997–2003	0.64	−0.18	0.60	0.70	2004–2015	0.68	−0.06	0.56	0.68
ST. Chikreng	Kampong Kdei	1997–2003	−1.96	−1.95	1.72	0.64	2004–2015	0.11	−0.89	0.94	0.48
ST. Siem Reap	Prasat Keo	1999–2003	0.63	−0.16	0.61	0.68	2004–2015	0.64	−0.02	0.60	0.65
ST. Sreng	Kralanh	1997–2003	0.67	−0.21	0.58	0.75	2004–2011	0.71	−0.27	0.54	0.79
ST. Mongkol Borey	Sisophon	1997–2003	0.43	−0.22	0.75	0.49	2004	0.37	−0.27	0.79	0.41
ST. Sangke	Battambang	1997–2003	0.32	−0.30	0.82	0.55	2004–2015	0.19	−0.62	0.90	0.70
ST. Dauntri	Prek Chik	1997–2003	−1.87	−2.26	1.69	0.35	2004, 2007–2008	−1.15	−1.40	1.47	0.35
ST. Pursat	Bac Trakuon	1995–2003	0.71	−0.09	0.54	0.71	2004–2015	0.65	0.01	0.59	0.64
ST. Baribo	Baribo	1998–2003	0.63	0.02	0.61	0.62	2004–2005	0.52	0.20	0.70	0.55

3.2. Changes in the Flow Regime

Future changes in river flow were analysed through the changes in rainfall as projected by the three GCMs and the medium-emissions scenarios RCP 6.0, by comparing the annual stream flow data between the baseline (1985–2005) and three future time horizons 2030s (2021–2040), 2060s (2051–2070), and 2090s (2081–2100) (Appendix A Figures A2 and A3). These projected hydrographs and percentage changes in the monthly flow showed a clear trend in changes. The magnitude of the changes varied, depending on the season, and most rivers showed flow reductions in the dry season for most GCMs and time horizons, with the exceptions being the Staung and Sreng Rivers. During the wet season (May–October), river flows were predicted to decrease for all time horizons, in particular, with the GISS-E2-R-CC model.

The potential effects of future climate change on 11 mean annual flows as generated by the outputs of the three GCMs (GFDL-CM3, GISS-E2-R-CC and IPSL-CM5A-MR) in three time-horizons, is shown as percentage changes (Table 5). The changes in the annual flow compared with the baseline annual flow for the baseline period (1985–2005) showed that the annual flows are projected to decline for most GCMs and time horizons. Among all of the rivers, Siem Reap faces significant flow reductions, ranging from 33% to 78%, while only the Chikreng indicated rising flows under the IPSL scenario for all time horizons (32% in 2030s, 12% in 2060s, and 51% in 2090s), and the Staung showed rising flows that varied from 2% to 53% for the GFDL and IPSL scenarios.

Table 5. Percentage changes in the mean annual flows for different climate scenarios, compared with baseline flows.

River Name	GCMs	2030s	2060s	2090s
		(2021–2040)	(2051–2070)	(2081–2100)
ST. Chinit	GFDL-CM3	−26	−28	−29
	GISS-E2-R-CC	−46	−50	−56
	IPSL-CM5A-MR	−26	−27	−25
ST. Sen	GFDL-CM3	−16	−16	−33
	GISS-E2-R-CC	−47	−40	−58
	IPSL-CM5A-MR	−17	−8	−33
ST. Staung	GFDL-CM3	6	10	53
	GISS-E2-R-CC	−27	−28	−13
	IPSL-CM5A-MR	32	29	2
ST. Chikreng	GFDL-CM3	7	−14	62
	GISS-E2-R-CC	−36	−42	4
	IPSL-CM5A-MR	32	12	51
ST. Siem Reap	GFDL-CM3	−51	−48	−40
	GISS-E2-R-CC	−78	−73	−68
	IPSL-CM5A-MR	−49	−40	−33
ST. Sreng	GFDL-CM3	−6	−38	−23
	GISS-E2-R-CC	−51	−56	−57
	IPSL-CM5A-MR	11	8	−12
ST. Mongkol Borey	GFDL-CM3	−12	−11	−2
	GISS-E2-R-CC	−22	−28	−34
	IPSL-CM5A-MR	−16	−13	−14
ST. Sangke	GFDL-CM3	−20	−18	−15
	GISS-E2-R-CC	−34	−37	−44
	IPSL-CM5A-MR	−26	−28	−31
ST. Dauntri	GFDL-CM3	−9	3	−4
	GISS-E2-R-CC	−25	−15	−28
	IPSL-CM5A-MR	−9	−15	−18

Table 5. Cont.

River Name	GCMs	2030s	2060s	2090s
		(2021–2040)	(2051–2070)	(2081–2100)
ST. Pursat	GFDL-CM3	−10	3	−7
	GISS-E2-R-CC	−23	−28	−38
	IPSL-CM5A-MR	−12	−14	−13
ST. Baribo	GFDL-CM3	−3	−9	2
	GISS-E2-R-CC	−17	−54	−66
	IPSL-CM5A-MR	−29	−7	−31

The projections for dry-season flows in the 2030s indicated significant flow declines in the Chinit, Sen, Sreng and Siem Reap rivers, varying from 61% to 97% for GISS-E2-R-CC, and flow decreases from 66% to 100% in the Sangke, Sreng, Chikreng and Baribo Rivers for IPSL-CM5A-MR. However, some rivers (Staung, Chikreng and Baribo) showed slight flow increases during the dry season, for GISS-E2-R-CC. In the wet season, in the 2030s, some rivers showed significant monthly flow declines, such as Sen (69%; GISS), Sreng (84%; IPSL-CM5A-MR), Siem Reap (−97%; GISS-E2-R-CC), Chikreng (87%; GISS) and Baribo (65%; IPSL-CM5A-MR), respectively. Some rivers showed monthly flow increases: Staung (39%; IPSL-CM5A-MR), Sreng (28%; IPSL-CM5A-MR), Dauntri (10%, IPSL-CM5A-MR), Chikreng (23%; GISS-E2-R-CC) and Baribo (7%; GISS-E2-R-CC).

3.3. Changes in Hydrological Extremes

Climate change has the potential to substantially alter river flow regimes, resulting in changes to extreme events, such as floods and droughts, especially Q_5 (high flow) and Q_{95} (low flow). (Tables 6 and 7, respectively). Both Q_5 and Q_{95} were extracted from flow duration curves, which were derived from simulated daily flows for all climate models in all projected periods (Figure 4).

Table 6. Percentage changes in Q_5 for the three GCMs in the three scenario periods.

River Name	Time Horizon	Baseline	GFDL-CM3		GISS-E2-R-CC		IPSL-CM5A-MR	
		Stream-Flow ^a	Stream-Flow ^a	% Change	Stream-Flow ^a	% Change	Stream-Flow ^a	% Change
ST.Chinit	2030s	225.6	185.6	−18	137.7	−39	182.3	−19
	2060s	225.6	177	−21	127.8	−43	189.9	−16
	2090s	225.6	178.8	−21	120.6	−46	198.7	−12
ST.Sen	2030s	794.9	756	−5	519.2	−35	760.9	−4
	2060s	794.9	697.9	−12	542.8	−32	830.6	4
	2090s	794.9	628.4	−21	378.9	−52	662	−17
ST.Staung	2030s	96.2	105.9	10	72.1	−25	120.6	25
	2060s	96.2	116.5	21	81.4	−15	121.4	26
	2090s	96.2	134.4	40	82.6	−14	106.6	11
ST.Chikreng	2030s	136.7	155.2	13	102.2	−25	178.5	31
	2060s	136.7	125.6	−8	98.4	−28	167.6	23
	2090s	136.7	186.9	37	145.4	6	200.3	46
ST.Siem Reap	2030s	24.5	15.2	−38	7.5	−69	16.5	−33
	2060s	24.5	15.7	−36	9.8	−60	20	−18
	2090s	24.5	17.9	−27	15.5	−37	22.5	−8
ST.Sreng	2030s	216.9	219.8	1	131.8	−39	257.5	19
	2060s	216.9	160.7	−26	125.1	−42	266.5	23
	2090s	216.9	195.4	−10	118.3	−45	255.2	18
ST.Mongkol Borey	2030s	65.2	60.2	−8	54.9	−16	61	−6
	2060s	65.2	58.6	−10	51	−22	62.8	−4
	2090s	65.2	66.1	1	49	−25	64.5	−1
ST.Sangke	2030s	289.4	261.8	−9	217.5	−25	249.8	−14
	2060s	289.4	264.9	−8	210	−27	250.5	−13
	2090s	289.4	279.9	−3	196.1	−32	248.5	−14

Table 6. Cont.

River Name	Time Horizon	Baseline	GFDL-CM3		GISS-E2-R-CC		IPSL-CM5A-MR	
		Stream-Flow ^a	Stream-Flow ^a	% Change	Stream-Flow ^a	% Change	Stream-Flow ^a	% Change
ST.Dauntri	2030s	39.9	37.2	-7	30.6	-23	37.1	-7
	2060s	39.9	41.1	3	33.1	-17	35.4	-11
	2090s	39.9	39.1	-2	28.6	-28	34.7	-13
ST.Pursat	2030s	252.9	238.4	-6	203.7	-19	234.1	-7
	2060s	252.9	264.6	5	192.8	-24	230.8	-9
	2090s	252.9	248.9	-2	170.4	-33	234	-7
ST.Baribo	2030s	46.7	47.8	2	43	-8	40.5	-13
	2060s	46.7	47.8	2	43	-8	40.5	-13
	2090s	46.7	49.6	6	22.8	-51	40.5	-13

^a The streamflow unit is in cubic meters per second (m³/s).

Table 7. Percentage changes in Q₉₅ for the three GCMs during the three time periods.

River Name	Time Horizon	Baseline	GFDL-CM3		GISS-E2-R-CC		IPSL-CM5A-MR	
		Stream-Flow ^a	Stream-Flow ^a	% Change	Stream-Flow ^a	% Change	Stream-Flow ^a	% Change
ST. Chinit	2030s	11.8	8.2	-30	4.1	-65	6.7	-43
	2060s	11.8	7.3	-38	3.9	-67	6.2	-48
	2090s	11.8	6.6	-44	3.2	-73	6.2	-47
ST. Sen	2030s	2.9	2.8	-4	1.7	-42	2.7	-5
	2060s	2.9	2.9	1	1.9	-35	2.6	-8
	2090s	2.9	2.3	-19	1.5	-46	1.8	-36
ST. Staung	2030s	0	0	0	0	0	0	0
	2060s	0	0	0	0	0	0	0
	2090s	0	0	0	0	0	0	0
ST. Chikreng	2030s	0	0	0	0	0	0	0
	2060s	0	0	0	0	0	0	0
	2090s	0	0	0	0	0	0	0
ST. Siem Reap	2030s	0.1	0	-67	0	-90	0	-64
	2060s	0.1	0	0	0	-93	0	-59
	2090s	0.1	0	-59	0	-95	0	-57
ST. Sreng	2030s	0	0	0	0	0	0	0
	2060s	0	0	0	0	0	0	0
	2090s	0	0	0	0	0	0	0
ST. Mongkol Borey	2030s	6.6	6	-10	5.2	-22	5.2	-22
	2060s	6.6	6.5	0	5	-24	5.6	-16
	2090s	6.6	6.5	-2	4	-39	4.8	-28
ST. Sangke	2030s	0.4	0.3	-28	0.2	-58	0.1	-63
	2060s	0.4	0.4	0	0.1	-65	0.2	-60
	2090s	0.4	0.4	2	0.1	-67	0.1	-75
ST. Dauntri	2030s	1.1	0.8	-23	0.6	-47	0.8	-24
	2060s	1.1	1.1	0	1	-9	0.7	-38
	2090s	1.1	0.8	-23	0.6	-40	0.6	-49
ST. Pursat	2030s	12.1	11.3	-7	9	-26	10.6	-13
	2060s	12.1	12.5	0	10.3	-15	10	-18
	2090s	12.1	11.3	-7	8.3	-31	9.3	-23
ST. Baribo	2030s	0.2	0.2	-3	0.1	-58	0	-80
	2060s	0.2	0.2	0	0	-93	0.1	-54
	2090s	0.2	0.3	42	0	-99	0	-86

^a Streamflow unit is cubic meters per second (m³/s).

The Q₅ values (high flows exceeded only 5% of the time) showed a decreasing trend for all rivers, and for most time horizons and GCMs (Table 6). During the 2030s time period, nine rivers (Chinit, Sen, Siem Reap, Mongkol Borey, Sangke, Dauntri, Pursat and Baribo) showed decreases in Q₅ from 4% to 69%, while two rivers (Staung and Chikreng) indicated increases from 1% to 31%, respectively. A decreasing trend was also evident for the 2060s time horizon for the three GCMs, particularly with GISS-E2-R-CC resulting in a 60% difference for Siem Reap. However, Staung, Chikreng and Sreng showed increases of 26%, 23% and 23%, respectively, for IPSL-CM5A-MR, while Baribo, Pursat and Dautri show increases of 2%, 5% and 3%, respectively, for GFDL. In the 2090s time period, Q₅ is predicted to increase only in the Chikreng River (for all GCMs), from 6% to 46%. The Sen River shows a reduction of 52% for GISS-E2-R-CC, while the Sambo, Chinit and Sreng Rivers show decreases of 51%, 46% and 45%, respectively. These results indicate that overall, future flood magnitudes would be reduced for all sub-basins under the GISS scenario over the majority of time horizons, and that reductions are also projected by the GFDL-CM3 and IPSL-CM5A-MR, for most sub-basins as well.

Q_{95} values (low flows or baseflows exceeding 95% of the time) decreased for all time periods under the GISS-E2-R-CC and IPSL-CM5A-MR climate models (Table 7). During the time period of the 2030s, baseflows were predicted to decrease in the Chinit, Siem Reap, Sangke, Baribo and Dautri Rivers by 65%, 90%, 58%, 58% and 47%, respectively under the GISS scenario; however, the Staung, Chirkeng and Sreng Rivers did not show any changes in baseflows. These decreases in baseflow (Q_{95}) would have implications for sustaining natural ecosystems and biodiversity during the dry season.

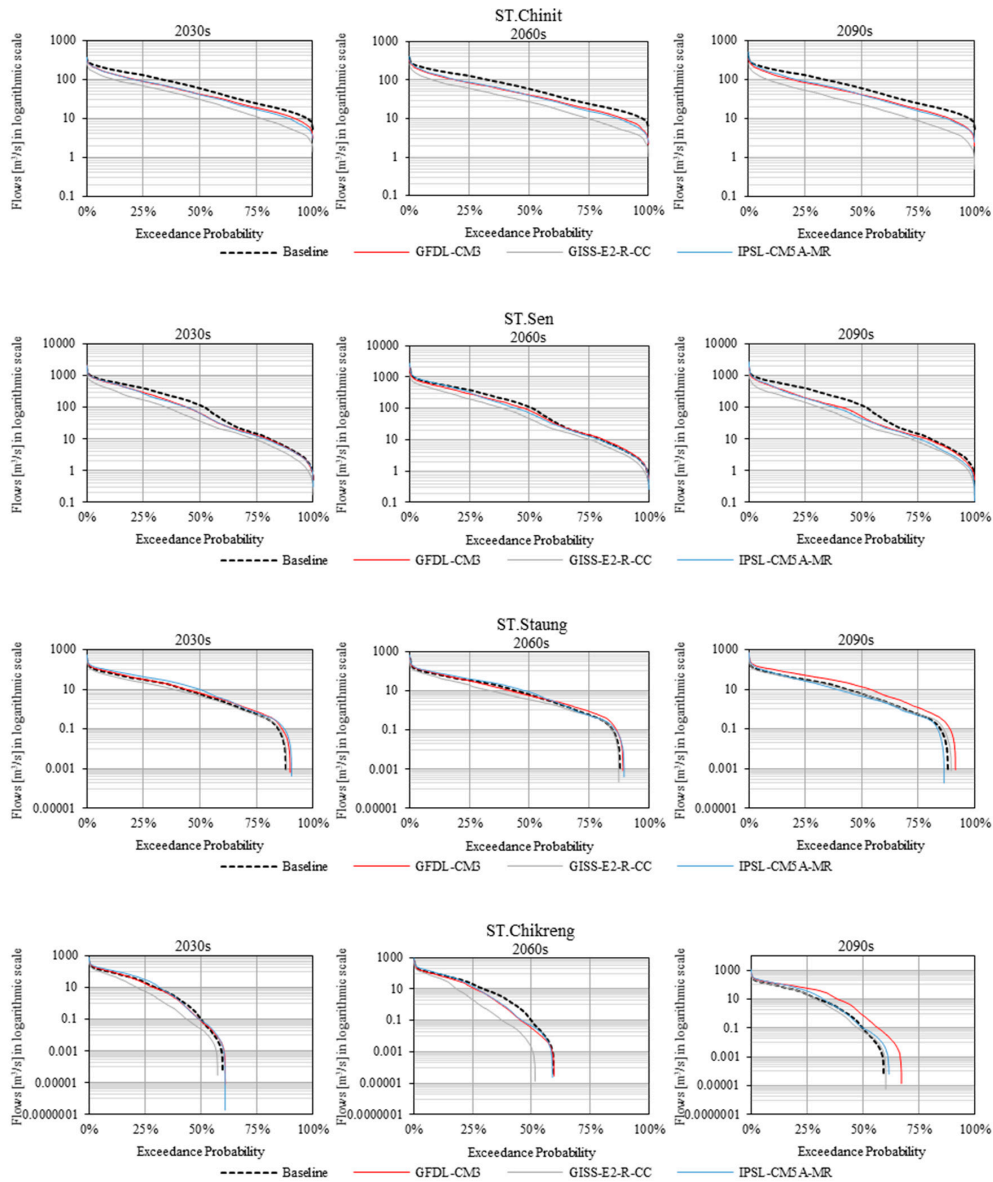


Figure 4. Cont.

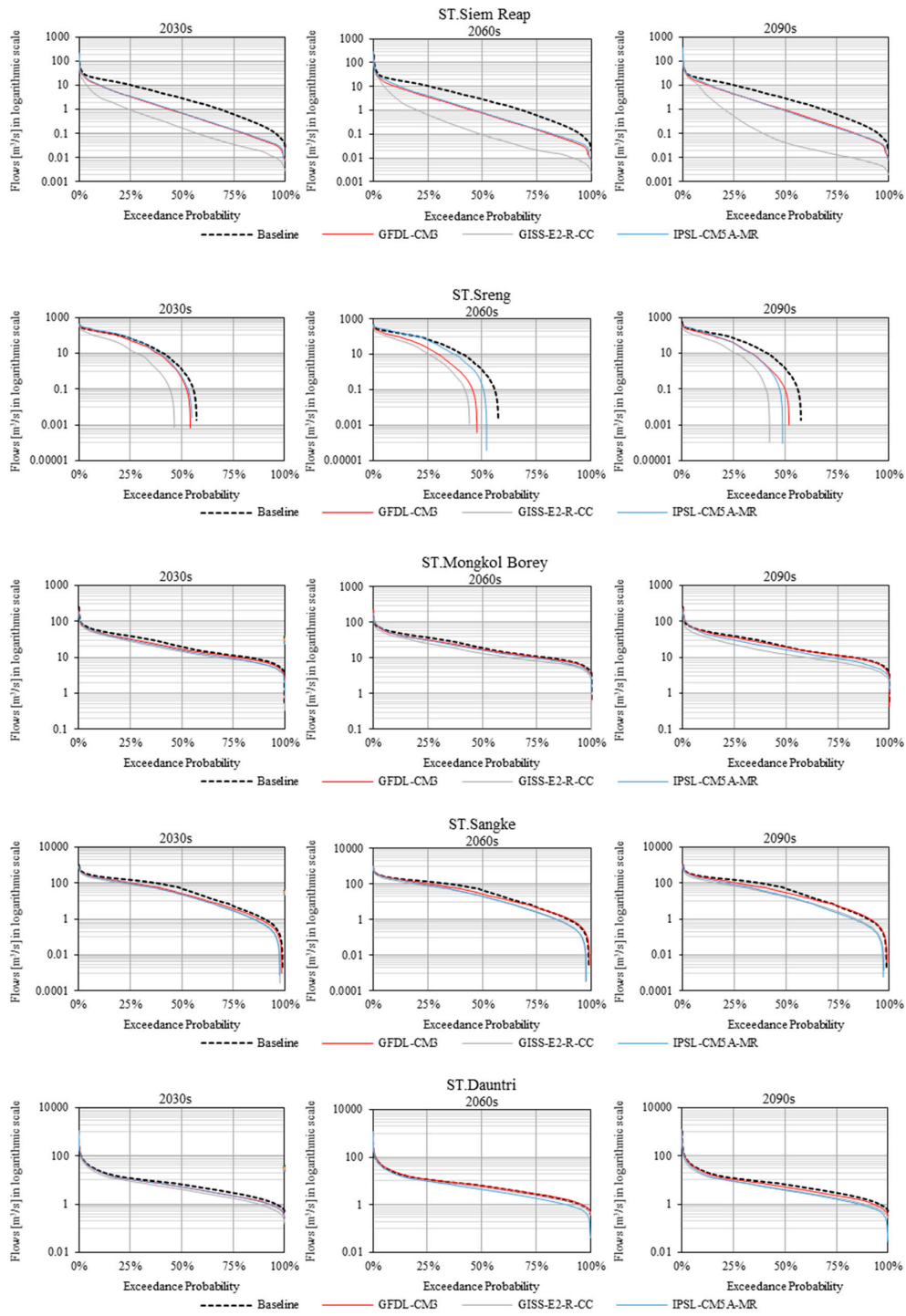


Figure 4. Cont.

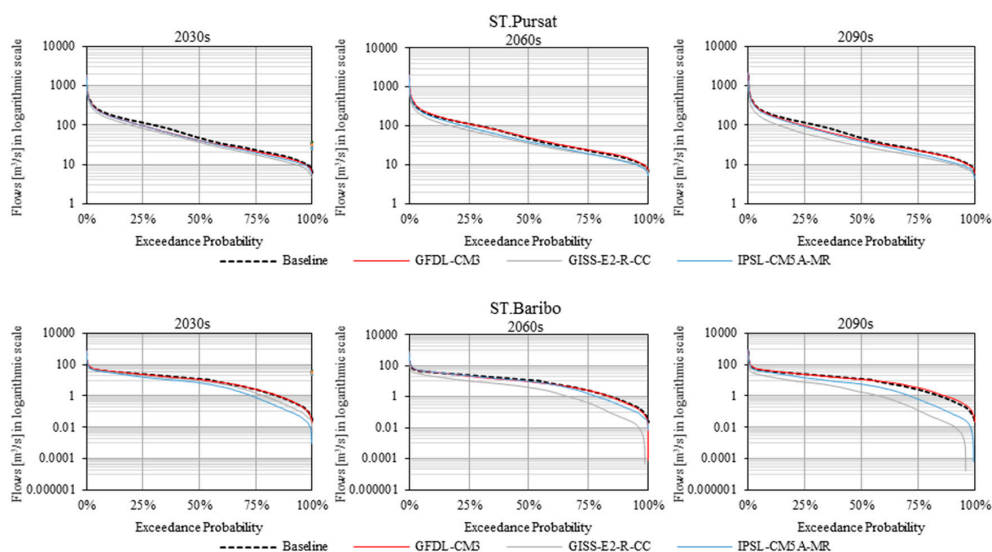


Figure 4. Flow duration curves of the baseline and for each GCM for three time horizons (2030s, 2060s, and 2090s).

4. Discussion

The river flow is a result of runoff from the catchment, which is affected by climate, as studied in this paper, but also other factors, such as land use. We expect that land-use changes will result in changes to the runoff regime. Land use has significantly changed in some sub-basins, notably in reduced forest cover. This study used a static 2003 land-use map for the whole simulation period, which would perforce a decrease in the accuracy of simulations, but they serve to isolate the differential effect of climate change on runoff. The relative paucity of the available ground truth data, and the rapid rate of land-use change makes it extremely difficult to forecast landuse with much certainty [39], but the potential effects of land-use change on runoff should be explored further. In addition, water withdrawals for irrigation and urban water supply were not included in the model, and these are increasing, so that they will likely have a much greater effect in the future. There are, of course, a number of other caveats with the analysis. The effects of hydrological model structure and parameter uncertainties were not considered. However, the effects of model parameter uncertainty have been shown [40] to be small, relative to the differences between climate scenarios. There are insufficient long-term rain gauges in the headwaters of the Tonle Sap tributaries, thus SWAT-assigned rainfall from the nearest stations, in some cases in Thailand. There is also considerable variability between climate model scenarios, particularly at the regional scale.

The subsequent assessment of potential impacts of climate change on river flow in these 11 sub-basins was thus conducted by comparing climate change simulations to the baseline scenario. Three General Circulation Models (GFDL-CM3, GISS-E2-R-CC, IPSL-CM5A-MR) for a medium-emissions scenario (RCP 6.0) were employed to project the future climate of the basin. Additionally, three time horizons, consisting of the near-term period (2030s), medium-term period (2060s) and long-term period (2090s) were considered in the investigation the potential impacts of climate change on river flow. The results of the climate change simulations on river flows revealed that it will be more likely that most sub-basins will experience extreme droughts, rather than floods. These results also suggest an increased risk of drought during both the dry and wet season, which would consequently impact future freshwater availability by decreasing both the annual and seasonal flow. The contribution of river flows from all tributaries into the Tonle Sap Lake will be decreasing, due to flow reduction, according to the simulation from the three GCMs and time horizons. These decreases are likely to be attributed to a change in the seasonal distribution of the rainfall, with drier and longer dry seasons, and lower precipitation occurring in the Lower Mekong Basin in the future climate projections, as reported by other studies of climate change in the region [14,41]. The analyses performed in this study are perhaps still too uncertain for detailed water management purposes. However, this

study gives insights into the sensitivity of this lake basin. In addition to the possible impacts of climate change, some basins such as Pursat, Sen and Sangke are faced with strong development pressures for hydropower and irrigation. Moreover, a decreasing trend of Q_5 and Q_{95} was projected by most GCMs for most future time periods, indicating that both the low flows and high flows will be lower than their baseline values. These results were in agreement with studies of future climate-change-induced changes in drought frequency for the Mekong River Basin, such as Hirabayashi et al. [42], which have projected an increase in drought days by 2100, and MRC (2010), who predicted an increase in drought frequency.

However, uncertainties that are associated with this type of climate change impact study should not be neglected when planning and designing additional water management measures. For instance, many studies have been conducted to assess the uncertainty in river flow projection that are associated with various GCMs under different emission scenarios in the Mekong River Basin [15,43]. They noted that the projections of river flow change are highly dependent upon the GCM used, with respect to the direction and magnitude of projected changes in precipitation produced by different GCMs. Indeed, the predictions of future river flow used constant land use and soil property data, unchanged from the baseline period, which is clearly not the case. Moreover, the effects of water infrastructure development projects (e.g., hydropower dams, irrigation schemes) coupled with deforestation, could have greater impacts on the water availability in the near-future (the next 20 to 30 years) than the direct effects of climate change. Therefore, the combined impacts of climate and land use change could significantly reduce river flows within the basin. Further studies are needed in order to assess the potential impacts of climate change that are associated with the future land use changes on river flow in the Tonle Sap Basin. Exploring the implications of water level changes in Tonle Sap Lake is beyond the scope of this study, but we expect that lower water levels would result in reduced a extent of the flooded lake, and likely a reduction in the productivity of the fisheries that depend upon large areas of inundation.

5. Conclusions

Our assessment of climate change effects on hydrological regimes in 11 sub-basins of the Tonle Sap Lake Basin indicate that annual and monthly river flows are likely to decrease in both the wet and dry seasons, for all time horizons (2030s, 2060s and 2090s), and a potential decrease in extreme river flows (Q_5 and Q_{95}). These reduced flood peaks and reduced base flows could threaten not only river ecosystems, but also socio-economic development, particularly for the agriculture sector.

This study provides water resources managers and policy makers with a wide range of water flow projections within the Tonle Sap basin, in the context of plausible climate change scenarios, while recognizing the high uncertainty in projections. Future climate change will have an important influence on water resources in the basin. To mitigate anticipated adverse effects will require more efficient methods to manage water resources, such as land cover management, the adoption of best management practices, water storage options and efficient agricultural irrigation systems.

Author Contributions: C.O. conducted the modelling, analysed the results and wrote the paper. T.A.C. supervised the research, advised on the methodologies, gave comments and corrected the manuscript. S.C. assisted in modelling and data processing from the model, M.G.K., M.E.A., T.P. gave comments and improved the manuscript.

Funding: This study was funded by a grant from the John D. and Catherine T. MacArthur Foundation through a project entitled “Increasing community and biodiversity resilience to development and climate-change based threats on the Tonle Sap Lake” in partnership with Conservation International via a subproject “Managing pressures from the development of dams, land use conversion, and climate change on riverine ecosystems of the Mekong’s Tonle Sap basin”, grant number 6001451. Dr. OEURNG Chantha was further supported by a Fulbright US-ASEAN Visiting Scholar Fellowship at the University of California, Berkeley, USA, and manuscript preparation was partially supported by the Collegium de Lyon—Institut des Etudes Avancées de l’Université de Lyon, the EURIAS Fellowship Programme, and the European Commission (Marie-Sklodowska-Curie Actions-COFUND Programme-FP7).

Acknowledgments: The authors would like to thank the Mekong River Commission for providing datasets, and particularly the MRC IKMP modelling team (Ornanong Vonnarart, Dat Nguyen Dinh and Sopheap Lim) for their modelling support. The authors would also like to thank the anonymous reviewers and the editor for providing valuable comments which helped improve this manuscript.

Conflicts of Interest: The authors declare no conflict of interest.

Appendix A

Table A1. Rating curve developed to estimate river flows [26] for the monitored water levels at the outlets of the 11 Tonle Sap sub-basins.

Sub-Basin	Rating Curve	Observed Discharge
ST. Chinit	$Q = 15.49 - 36.8088 \times H_{KgThom} + 36.3032 \times H_{KgThom}^2 - 8.5957 \times H_{KgTmar}^3 + 0.7869 \times H_{KgTmar}^4$	1997–2015
ST. Sen	$Q = 0.000013 \times (H_{KgThom} - 1.21)^{6.8178} \times F^{0.72};$ where, $F = H_{KgThom} - H_{KgLuong}$	1995–2015
ST. Staung	$Q = 0.8554 \times H_{KgChen}^{2.7794} \times F^{0.5};$ where, $F = H_{KgChen} - H_{KgLuong} + 7.0$	1997–2015
ST. Chikreng	$Q = 0.1017 \times H_{KgKdey}^{3.3034} \times F^{0.5};$ where, $F = H_{KgChen} - H_{KgKdey} + 7.0$	1997–2010
ST. Siem Reap	$Q = 4.1059 \times (H_{UntacBridge} - 0.0936)^2$	1997–2010
ST. Sreng	$Q = 0.01299 \times H_{Kralanh}^{4.3665} \times F^{0.5};$ where, $F = H_{Kralanh} - H_{BakPrea} + 4.0$	1997–2010
ST. Mongol Borey	$Q = y \times (f + 6.09)^{0.69}$ $y = -0.5665 + 2.212 \times H_{MongolBorey} - 0.8243 \times H_{MongolBorey}^2 - 0.1796 \times H_{MongolBorey}^3$ $F = H_{MongolBorey} - H_{BakPrea} + 6.0$	1997–2010
ST. Sangke	$Q = y \times (F + 0.3)^{0.18}$ $y = -28.2541 + 33.8995 \times H_{Battambang} - 9.5551 \times H_{Battambang}^2 - 0.8092 \times H_{Battambang}^3$ $F = H_{MongolBoery} - H_{BakPrea}$	1997–2015
ST. Dauntri	$Q = 12.4 \times (H_{MaungRussey} - 1.2439)^2$	1997–2010
ST. Pursat	$Q = 25.5 \times (H_{BakTrakuon} - 0.0856)^2$	1995–2015
ST. Baribo	$Q = 37.1593 \times H_{Baribor}^{1.6195}$	1997–2010

Table A2. SWAT model-calibrated parameter values for all 11 river sub-basins of the Tonle Sap Lake.

Parameters	Min Value	Max Value	Calibrated Value										
			Chinit	Sen	Pursat	Sangke	Staung	Sreng	Siem Reap	Mongkol Borey	Chikreng	Dauntri	Baribo
v_GW_DELAY.gw	0	500	68	24	80	1.5	35	42	8	55	35	16	25
v_ALPHA_BF.gw	0	1	0.13	0.2	0.4	0.7	0.5	0.4	0.04	0.6	0.5	0.16	0.1
v_GWQMN.gw	0	5000	0	500	1	500	500	398	500	5	500	0.01	1
v_GW_REVP.gw	0.02	0.2	0.2	0.02	0.2	0.02	0.2	0.02	0.2	0.2	0.2	0.2	0.2
v_REVP.gw	0	500	500	501	2	1500	475	501	501	6	475	0.02	2
v_RCHRG_DP.gw	0	1	0.4	0.4	0.2	0.0001	0.4	0.24	0.4	0.4	0.4	0	0.4
v_LT_TIME.hur	0	180	0.01	0.1	180	0.3	10	100	150	30	10	19.2	0.8
v_SLSOIL.hur	0	150	0.3	1	150	150	0.35	150	100	0.3	0.35	0.4	70
v_CANMX.hur	0	1	7	7	20	0	5	4.5	10.5	5	5	20	7
v_ESCO.hur	0	1	0.7	0.7	0.7	1	0.7	0.7	0.7	1	0.7	0.79	1
v_CH_N2.rte	0	0.3	0.2	0.18	0.2	0.03	0.2	0.2	0.2	0.2	0.2	0.2	0.2
v_CH_K2.rte	0	500	10	2.5	10	9	10	10	-	-	-	-	-
v_ALPHA_BNK.rte	0	1	-	-	-	-	-	-	-	-	-	-	-
v_CH_N1.sub	0.01	30	0.12	0.02	0.2	0.001	0.2	0.2	0.02	0.2	0.2	0.2	0.2
v_CH_K1.sub	0	300	10	10	10	0.013	5	-	-	-	-	-	-
r_CN2.mgt	-25%	25%	-	0.05	-	-	-	-	-	-	-	-	-
r_SOL_AWC.sol	-25%	25%	-	-0.05	-	-	-	-	-	-	-	-	-
v_SOL_BD.sol	0.9	2.5	-	-	-	-	-	-	-	-	-	-	-
v_SOL_K.sol	0	2000	-	-	-	-	-	-	-	-	-	-	-

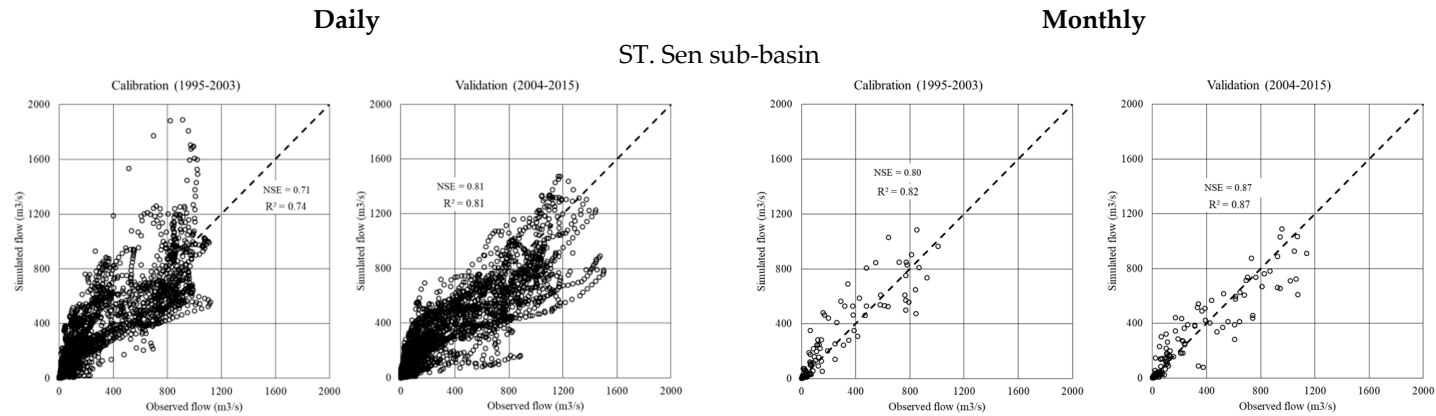


Figure A1. Cont.

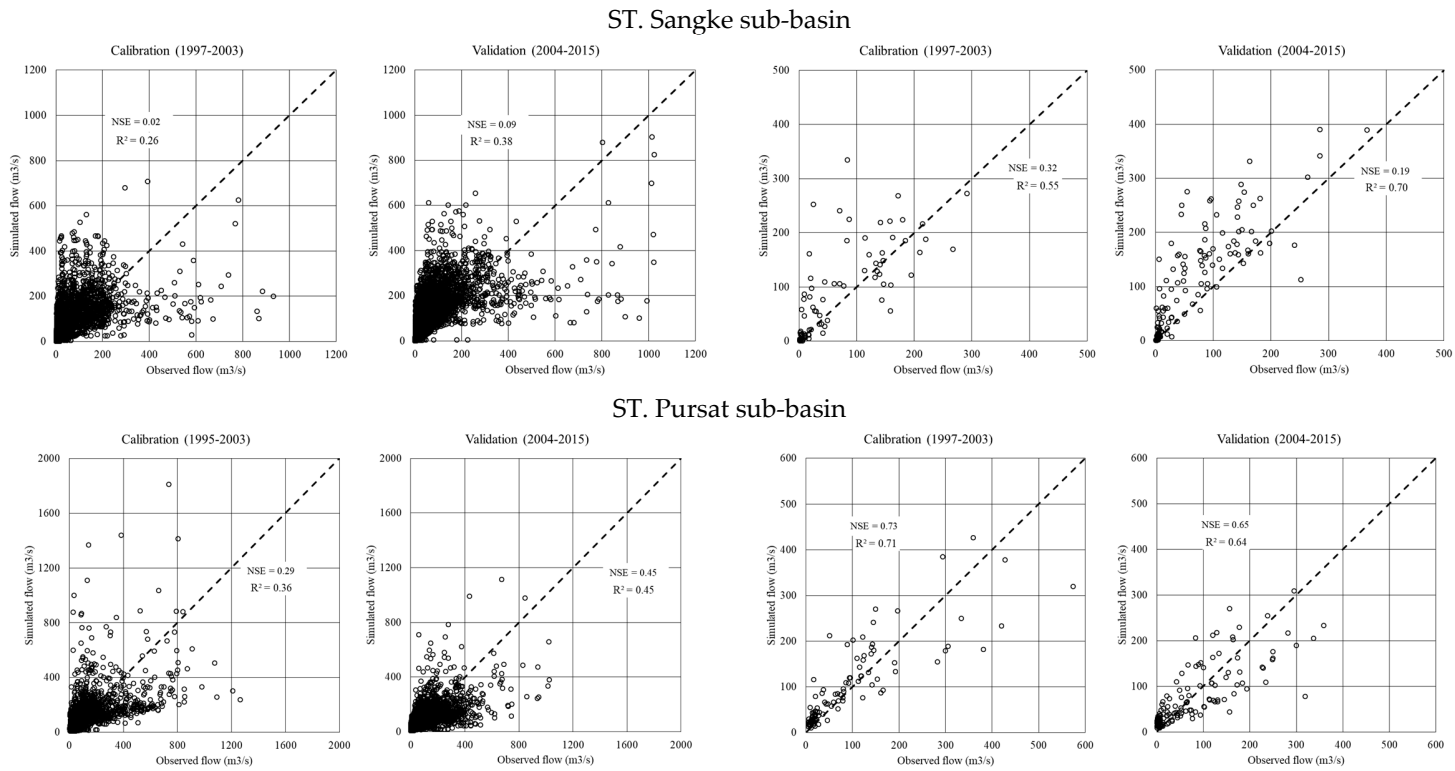


Figure A1. Scatter plots comparing between the observed and simulated river flows in selected sub-basins (ST. Sen, ST. Sangke, ST. Pursat) during calibration and validation.

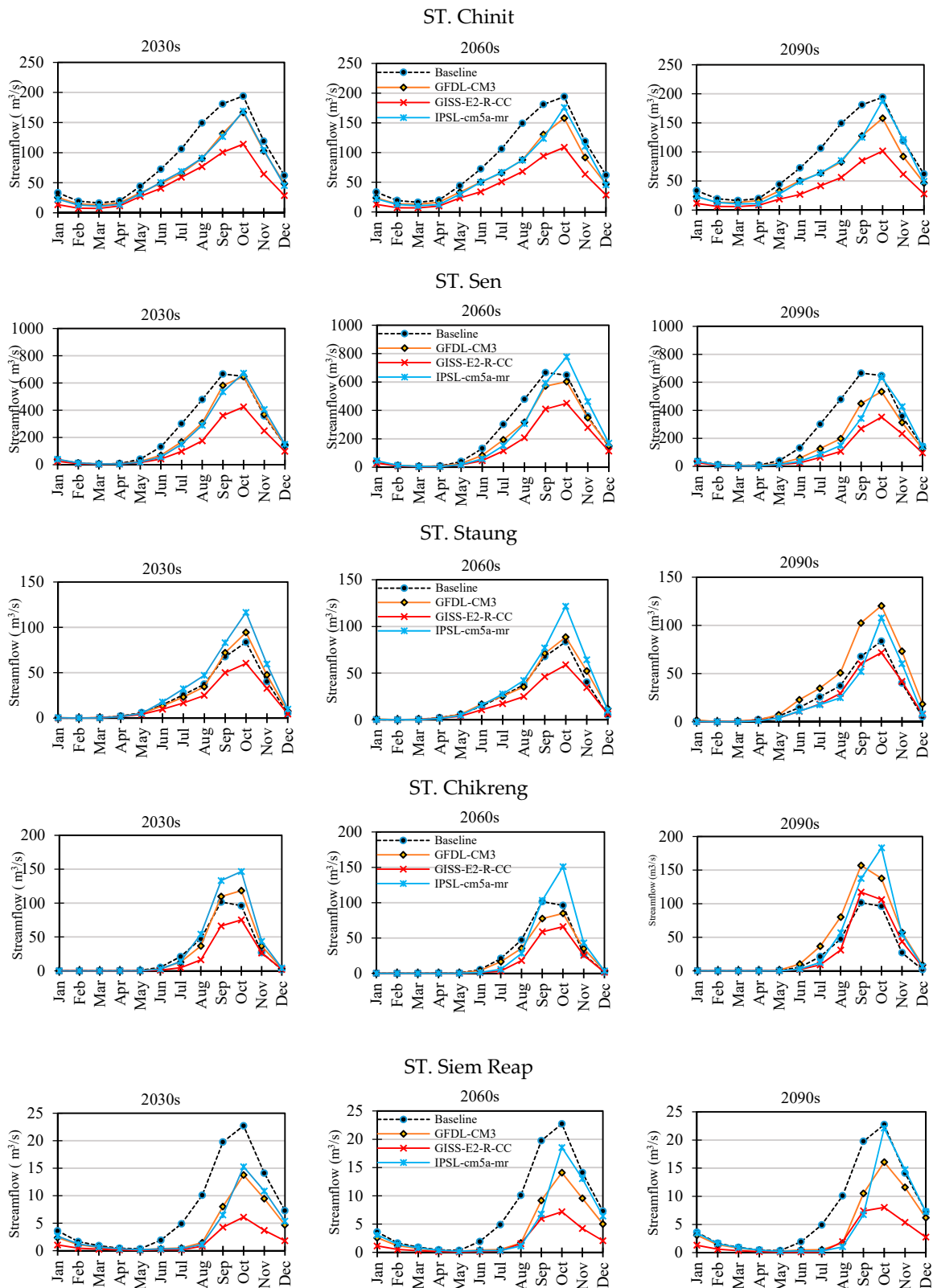


Figure A2. Cont.

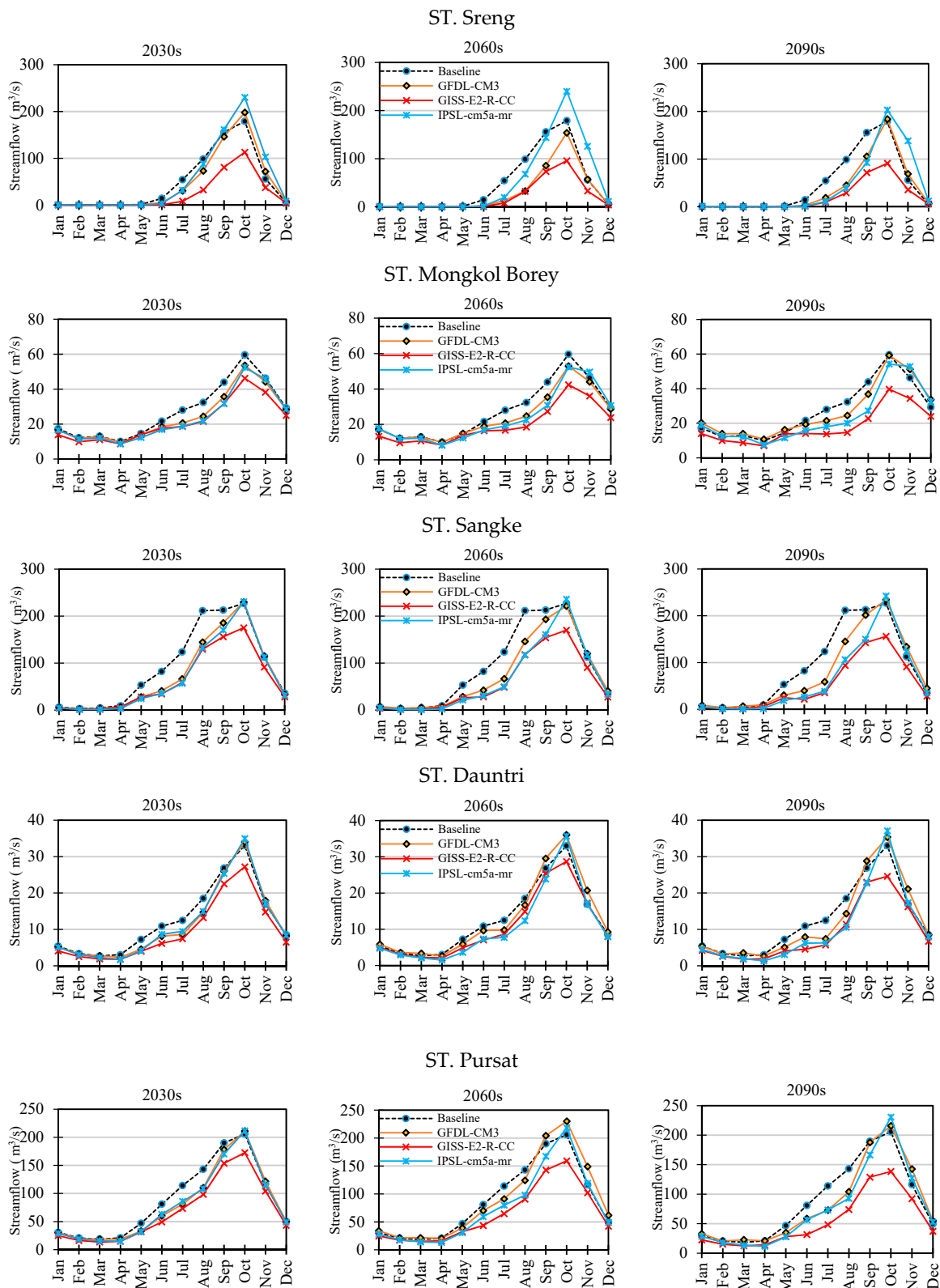


Figure A2. Cont.

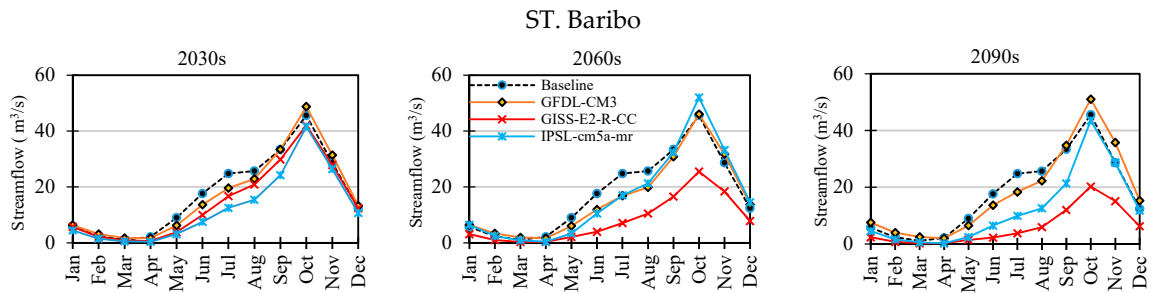


Figure A2. Mean monthly baseline river flows and 2030s, 2060s, and 2090s climate change scenario flows.

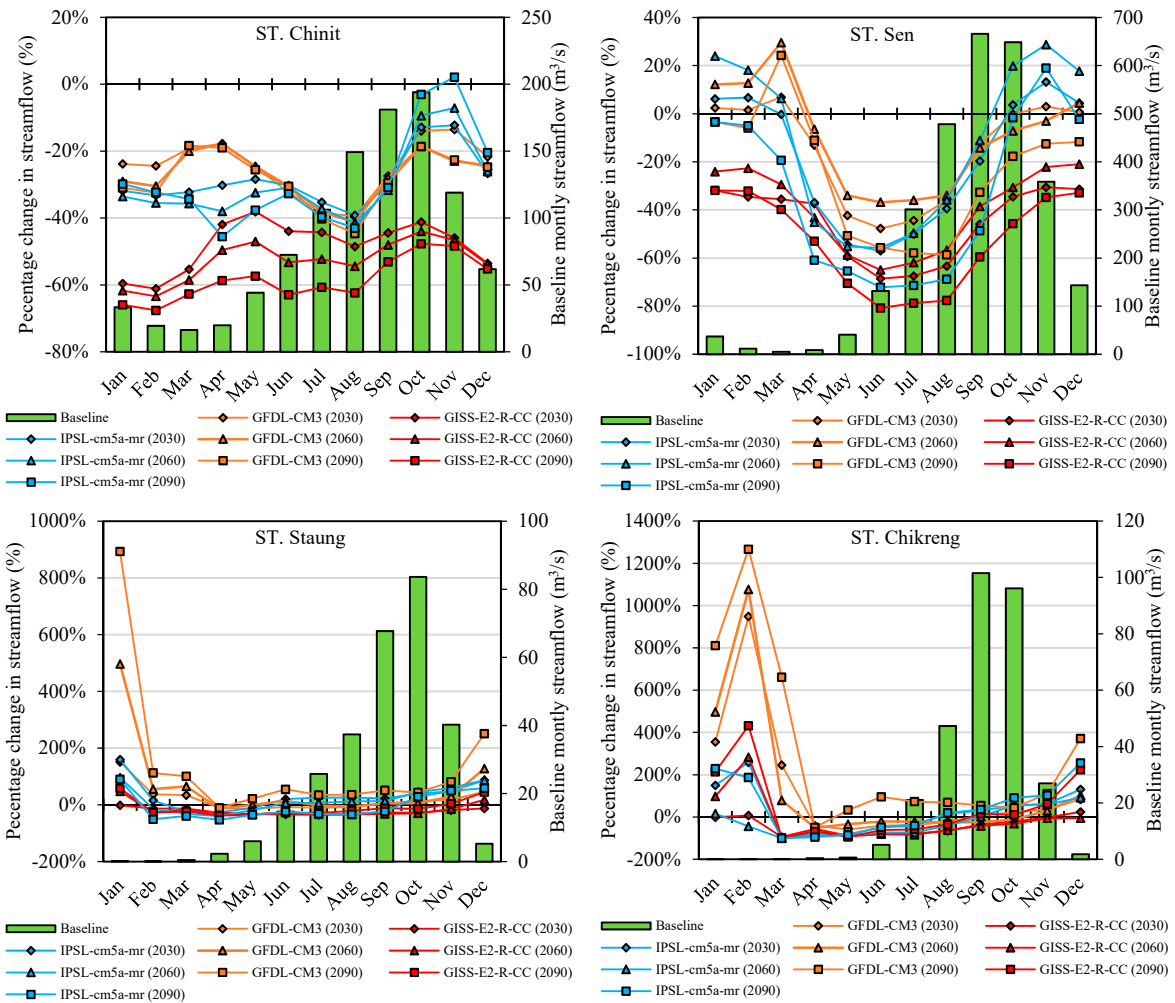


Figure A3. Cont.

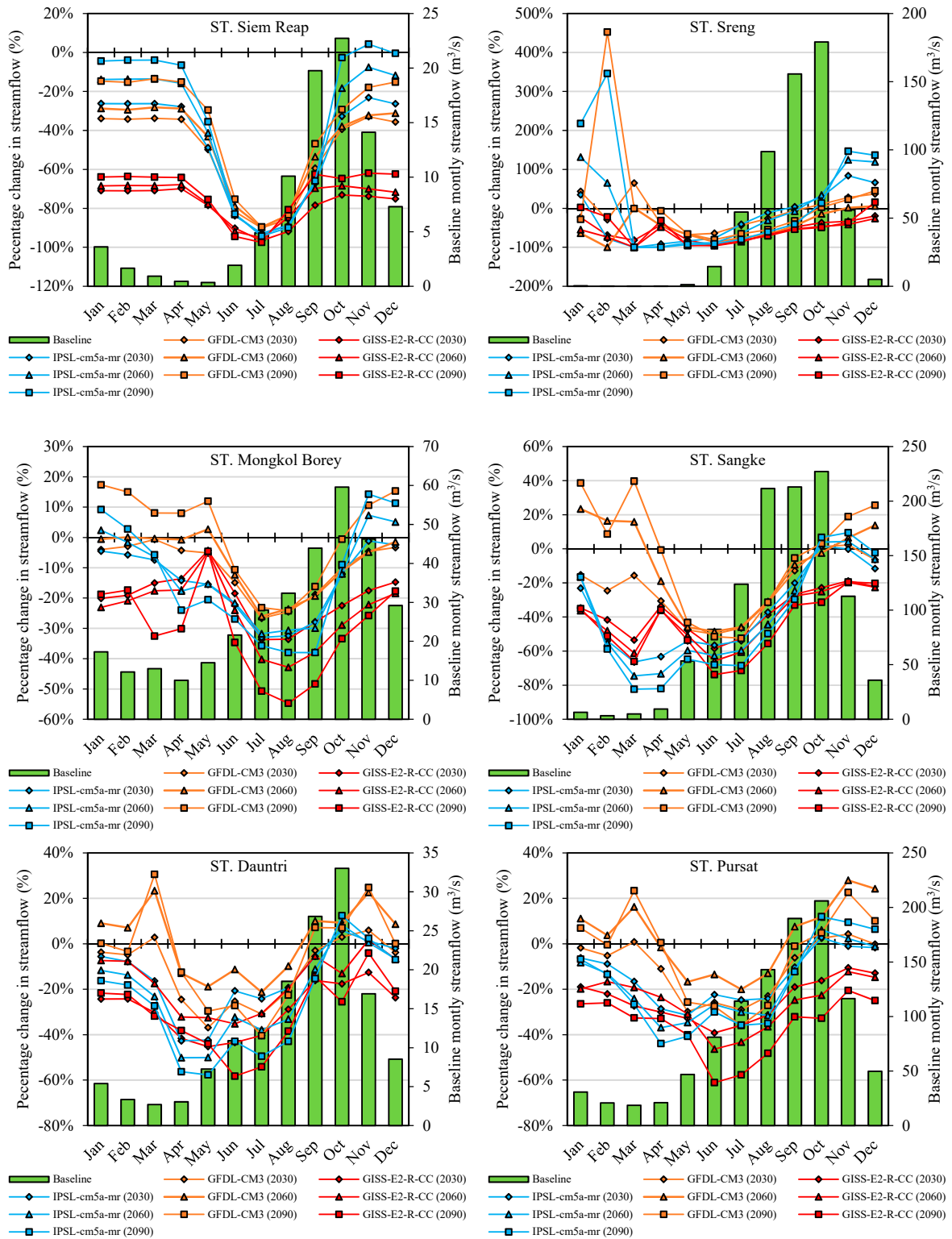


Figure A3. Cont.

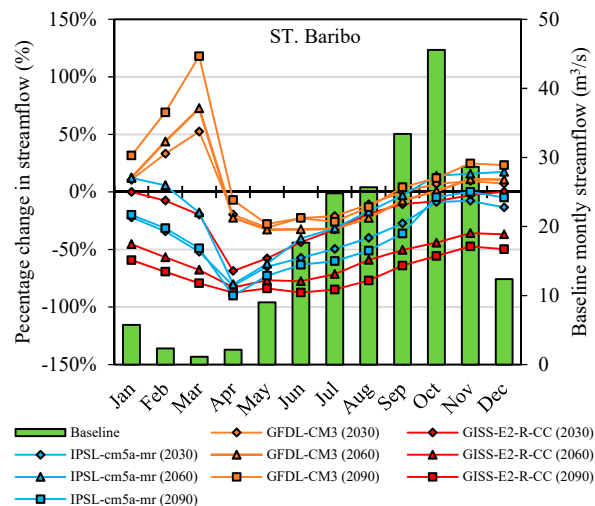


Figure A3. Baseline monthly streamflows and percent changes in mean monthly river flows from baseline for the 2030s, 2060s and 2090s climate change scenarios.

References

- Dhar, S.; Mazumdar, A. Impacts of climate change under the threat of global Warming for an agricultural watershed of the Kangsabati River. *Int. J. Civ. Environ. Eng.* **2009**, *1*. [[CrossRef](#)]
- Intergovernmental Panel on Climate Change (IPCC). *Climate Change 2013: The Physical Science Basis. Contribution of Working Group I to the Fifth Assessment Report of the Intergovernmental Panel on Climate Change*; Cambridge University Press: Cambridge, UK; New York, NY, USA, 2013.
- Huo, A.; Li, H. Assessment of climate change impact on the stream-flow in a typical debris flow watershed of Jianzhuangcuan catchment in Shaanxi Province, China. *Environ. Earth Sci.* **2013**, *69*, 1931–1938. [[CrossRef](#)]
- Lirong, S.; Jianyun, Z. Hydrological response to climate change in Beijiang River Basin based on the SWAT model. *Procedia Eng.* **2012**, *28*, 241–245. [[CrossRef](#)]
- Bates, B.; Kundzewicz, Z.; Wu, S. *Climate Change and Water—IPCC Technical Paper VI*; Intergovernmental Panel on Climate Change: Geneva, Switzerland, 2008.
- Intergovernmental Panel on Climate Change (IPCC). *Climate Change 2014: Synthesis Report. Contribution of Working Groups I, II and III to the Fifth Assessment Report of the Intergovernmental Panel on Climate Change*; IPCC: Geneva, Switzerland, 2014.
- Van Vuuren, D.P.; Edmonds, J.; Kainuma, M.; Riahi, K.; Thomson, A.; Hibbard, K.; Hurtt, G.C.; Kram, T.; Krey, V.; Lamarque, J.-F.; et al. The representative concentration pathways: An overview. *Clim. Chang.* **2011**, *109*, 5. [[CrossRef](#)]
- Young, R.; Onstad, C.; Bosch, D.; Anderson, W. AGNPS: A nonpoint-source pollution model for evaluating agricultural watersheds. *J. Soil Water Conserv.* **1989**, *44*, 168–173.
- Bicknell, B.R.; Imhoff, J.C.; Kittle, J.L., Jr.; Donigian, A.S., Jr.; Johanson, R.C. *Hydrological Simulation Program-FORTRAN. User's Manual for Release 11*; US EPA: Athens, Greece, 1996.
- Danish Hydraulic Institute (DHI). *MIKE SHE WM—Water Movement Module, A Short Description*; Danish Hydraulic Institute: Hørsholm, Denmark, 1993.
- Arnold, J.G.; Raghavan, S.; Ranjan, S.M.; Jimmy, R.W. Large area hydrologic modeling and assessment part I: Model development. *Jawra J. Am. Water Resour. Assoc.* **1998**, *34*, 91–101. [[CrossRef](#)]
- Williams, J.; Izaurralde, R. *Agricultural Policy/Environmental Extender Model Theoretical Documentation*; Blackland Research and Extension Center: Temple, TX, USA, 2008.
- Gassman, P.W.; Arnold, J.J.; Srinivasan, R.; Reyes, M. The worldwide use of the SWAT Model: Technological drivers, networking impacts, and simulation trends. In *Proceedings of the 21st Century Watershed Technology: Improving Water Quality and Environment Conference Proceedings*, EARTH University, Mercedes, Costa Rica, 21–24 February 2010; p. 1.

14. Piman, T.; Cochrane, T.A.; Arias, M.E.; Dat, N.D.; Vonnarart, O. Managing Hydropower Under Climate Change in the Mekong Tributaries. In *Managing Water Resources under Climate Uncertainty: Examples from Asia, Europe, Latin America, and Australia*; Shrestha, S., Anal, A.K., Salam, P.A., van der Valk, M., Eds.; Springer International Publishing: Cham, Switzerland, 2014; pp. 223–248. [[CrossRef](#)]
15. Shrestha, B.; Cochrane, T.A.; Caruso, B.S.; Arias, M.E.; Piman, T. Uncertainty in flow and sediment projections due to future climate scenarios for the 3S Rivers in the Mekong Basin. *J. Hydrol.* **2016**, *540*, 1088–1104. [[CrossRef](#)]
16. Oeurng, C.; Thomas, A.C.; Mauricio, E.A.; Bikesh, S.; Thanapon, P. Assessment of changes in riverine nitrate in the Sesan, Srepok and Sekong tributaries of the Lower Mekong River Basin. *J. Hydrol. Regional Stud.* **2016**, *8*, 95–111. [[CrossRef](#)]
17. Shrestha, S.; Shrestha, M.; Babel, M.S. Modelling the potential impacts of climate change on hydrology and water resources in the Indrawati River Basin, Nepal. *Environ. Earth Sci.* **2016**, *75*, 280. [[CrossRef](#)]
18. Giang, P.Q.; Toshiki, K.; Sakata, M.; Kunikane, S.; Vinh, T.Q. Modelling climate change impacts on the seasonality of water resources in the upper Ca River watershed in Southeast Asia. *Sci. World J.* **2014**, *279135*, 279135. [[CrossRef](#)]
19. Ligaray, M.; Kim, H.; Sthiannopkao, S.; Lee, S.; Cho, K.H.; Kim, J.H. Assessment on hydrologic response by climate change in the Chao Phraya River Basin, Thailand. *Water* **2015**, *7*, 6892–6909. [[CrossRef](#)]
20. Zhou, J.; He, D.; Xie, Y.; Liu, Y.; Yang, Y.; Sheng, H.; Guo, H.; Zhao, L.; Zou, R. Integrated SWAT model and statistical downscaling for estimating streamflow response to climate change in the Lake Dianchi watershed, China. *Stoch. Environ. Res. Risk Assess.* **2015**, *29*, 1193–1210. [[CrossRef](#)]
21. MOE and UNDP. *Cambodia Human Development Report 2011 Building Resilience: The Future of Rural Livelihoods in the Face of Climate Change*; Ministry of Environment: Phnom Penh, Cambodia, 2011.
22. Piman, T.; Cochrane, T.A. Assessment of flow changes from the operation of dams in the Mekong basin. *Int. J. Hydropower Dams* **2013**, *20*, 44–49.
23. Cochrane, T.A.; Arias, M.E.; Piman, T. Historical impact of water infrastructure on water levels of the Mekong River and the Tonle Sap system. *Hydrol. Earth Syst. Sci.* **2014**, *18*, 4529–4541. [[CrossRef](#)]
24. Lu, X.; Kummu, M.; Oeurng, C. Reappraisal of sediment dynamics in the Lower Mekong River, Cambodia. *Earth Surf. Process. Landf.* **2014**, *39*, 1855–1865. [[CrossRef](#)]
25. Hoang, P.; Lauri, P.; Kummu, M.; Koponen, J.; Van Vliet, M.T.; Supit, I.; Leemans, H.; Kabat, P.; Ludwig, F. Mekong River flow and hydrological extremes under climate change. *Hydrol. Earth Syst. Sci. Discuss.* **2016**, *20*, 3027–3041. [[CrossRef](#)]
26. Kummu, M.; Tes, S.; Yin, S.; Adamson, P.; Józsa, J.; Koponen, J.; Richey, J.; Sarkkula, J. Water balance analysis for the Tonle Sap Lake–floodplain system. *Hydrol. Process.* **2014**, *28*, 1722–1733. [[CrossRef](#)]
27. Japan International Cooperation Agency (JICA). *Land Use Map of Cambodia*; JICA: Tokyo, Japan, 2002.
28. Arias, M.E.; Cochrane, T.A.; Kummu, M.; Lauri, H.; Holtgrieve, G.W.; Koponen, J.; Piman, T. Impacts of hydropower and climate change on drivers of ecological productivity of Southeast Asia’s most important wetland. *Ecol. Model.* **2014**, *272*, 252–263. [[CrossRef](#)]
29. Sabo, J.L.; Ruhi, A.; Holtgrieve, G.W.; Elliott, V.; Arias, M.E.; Ngor, P.B.; Räsänen, T.A.; Nam, S. Designing river flows to improve food security futures in the Lower Mekong Basin. *Science* **2017**, *358*, eaao1053. [[CrossRef](#)] [[PubMed](#)]
30. Neitsch, S.L.; Arnold, J.G.; Kiniry, J.R.; Williams, J.R. *Soil and Water Assessment Tool Theoretical Documentation Version 2009*; Texas Water Resources Institute: College Station, TX, USA, 2011.
31. Arnold, J.G.; Allen, P.M.; Bernhardt, G. A comprehensive surface-groundwater flow model. *J. Hydrol.* **1993**, *142*, 47–69. [[CrossRef](#)]
32. Priestley, C.; Taylor, R. On the assessment of surface heat flux and evaporation using large-scale parameters. *Mon. Weather Rev.* **1972**, *100*, 81–92. [[CrossRef](#)]
33. Monteith, J.L. Evaporation and environment. *Sympos. Soc. Exp. Biol.* **1965**, *19*, 205–234.
34. Hargreaves, G.; Samani, Z.A. Reference Crop Evapotranspiration from Temperature. *Appl. Eng. Agric.* **1985**, *1*, 96–99. [[CrossRef](#)]
35. Mekong River Commission (MRC). *Technical Reference Report SWAT Model (Baseline 2007), Application in Mekong River Basin*; MRC: Phnom Penh, Cambodia, 2014.
36. Abbaspour, K.C. *SWAT-CUP 2012: SWAT calibration and Uncertainty Programs—A User Manual*; Swiss Federal Institute of Aquatic Science and Technology: Dübendorf, Switzerland, 2012.

37. Nash, J.E.; Sutcliffe, J.V. River flow forecasting through conceptual models part I—A discussion of principles. *J. Hydrol.* **1970**, *10*, 282–290. [[CrossRef](#)]
38. Mekong River Commission (MRC). *1st Draft Report on Defining Basin-Wide Climate Change Scenarios for the Lower Mekong Basin*; Mekong River Commission: Vientiane, Laos, 2015.
39. Wang, Z.; Ficklin, D.L.; Zhang, Y.; Zhang, M. Impact of climate change on streamflow in the arid Shiyang River Basin of northwest China. *Hydrol. Process.* **2012**, *26*, 2733–2744. [[CrossRef](#)]
40. Arnell, N. Uncertainty in the relationship between climate forcing and hydrological response in UK catchments. *Hydrol. Earth Syst. Sci.* **2011**, *15*, 897–912. [[CrossRef](#)]
41. Mekong River Commission (MRC). *State of the Basin Report*; Mekong River Commission: Vientiane, Laos, 2010.
42. Hirabayashi, Y.; Kanae, S.; Emori, S.; Oki, T.; Kimoto, M. Global projections of changing risks of floods and droughts in a changing climate. *Hydrol. Sci. J.* **2008**, *53*, 754–772. [[CrossRef](#)]
43. Kingston, D.; Thompson, J.R.; Kite, G. Uncertainty in climate change projections of discharge for the Mekong River Basin. *Hydrol. Earth Syst. Sci.* **2011**, *15*, 1459–1471. [[CrossRef](#)]



© 2019 by the authors. Licensee MDPI, Basel, Switzerland. This article is an open access article distributed under the terms and conditions of the Creative Commons Attribution (CC BY) license (<http://creativecommons.org/licenses/by/4.0/>).